Flight Acoustic Testing and Data Acquisition For the Rotor Noise Model (RNM)

David A. Conner
Aerospace Engineer
U.S. Army AFDD-JRPO, AMRDEC, RDECOM
Hampton, Virginia
d.a.conner@larc.nasa.gov

Casey L. Burley
Aerospace Technologist
NASA Langley Research Center
Hampton, Virginia
c.l.burley@larc.nasa.gov

Charles D. Smith
Aeronautical Staff Engineer
Lockheed Martin Engineering and Sciences Company
Hampton, Virginia
c.d.smith@larc.nasa.gov

Abstract

Two acoustic flight tests have been conducted on a remote test range at Eglin Air Force Base in the panhandle of Florida. The first was the "Acoustics Week" flight test conducted in September 2003. The second was the NASA Heavy Lift Rotorcraft Acoustics Flight Test conducted in October-November 2005. Benchmark acoustic databases were obtained for a number of rotorcraft and limited fixed wing vehicles for a variety of flight conditions. The databases are important for validation of acoustic prediction programs such as the Rotorcraft Noise Model (RNM), as well as for the development of low noise flight procedures and for environmental impact assessments. An overview of RNM capabilities and a detailed description of the RNM/ART (Acoustic Repropagation Technique) process are presented. The RNM/ART process is demonstrated using measured acoustic data for the MD600N. The RNM predictions for a level flyover speed sweep show the highest SEL noise levels on the flight track centerline occurred at the slowest vehicle speeds. At these slower speeds, broadband noise content is elevated compared to noise levels obtained at the higher speeds. A descent angle sweep shows that, in general, ground noise levels increased with increasing descent rates. Vehicle orientation in addition to vehicle position was found to significantly affect the RNM/ART creation of source noise semi-spheres for vehicles with highly directional noise characteristics and only mildly affect those with weak acoustic directionality. Based on these findings, modifications are proposed for RNM/ART to more accurately define vehicle and rotor orientation.

Introduction

The capability to predict rotorcraft ground noise contours is important in determining and assessing the environmental noise impact. The noise generated by rotorcraft can limit their usage and restrict operations, particularly near cities and populated regions. Rotorcraft noise tends to have strong impulsive and directional characteristics compared to fixed wing aircraft. Source noise levels can vary significantly depending on the vehicle design, and on the flight condition. For low speed descent, where blade vortex interaction (BVI) noise may be present, the noise levels can be on the order of 10-20 dB higher than for level flight or for a climb condition for which BVI is minimal or non-existent. In addition, the propagation effects on the rotorcraft source noise are strongly dependent on the source frequency and on atmospheric and terrain conditions. All these aspects of rotorcraft noise contribute to the complexity of determining and characterizing ground noise exposure due to rotorcraft operations. It is, therefore, important to accurately characterize and

Presented at the American Helicopter Society 62nd Annual Forum, Phoenix, AZ, May 9-11, 2006.

understand these effects in order to determine techniques to reduce the radiated noise.

The two primary approaches commonly used to reduce rotorcraft noise are to make vehicle design modifications and/or to make changes in operational flight procedures. Design changes typically require a significant development period, often requiring high production costs and expensive recertification. Since rotorcraft noise is highly directional and is a strong function of the operating condition, low noise flight procedures can often be implemented to achieve significant noise reductions at a lower cost than new design efforts. Measurement and prediction capabilities to develop low noise procedures have received much attention over the last 10 years. (Refs. 1-8). In all of these efforts, acoustic and vehicle state information from flight test databases were used to assess and/or design low noise flight procedures. In Refs. 1-4, acoustic footprints were measured for a large range of flight conditions, including approach, takeoff, and level flyovers. These measured databases were used to demonstrate noise abatement flight procedures and to further develop methods to predict the low noise procedures. In Refs. 3-7, the capability to predict low noise procedures from measured flight acoustic databases are presented and demonstrated. The success of each effort is shown to be dependent on not only the quality and density of the acoustic measurements, but also on the ability to simultaneously measure the acoustics, the vehicle operating condition (airspeed, rate of descent, rotor speed, rotor tilt, *etc.*), the vehicle position and orientation, and the environmental conditions.

A team composed of researchers from the NASA Langley Research Center (LaRC), the U.S. Army's Aeroflightdynamics Directorate, Joint Research Program Office, (AFDD-JRPO), and Wyle Laboratories has developed the Rotor Noise Model (Ref 8) to predict and develop low noise procedures and to assess the environmental impact of rotorcraft operations. RNM utilizes a database of source noise semi-spheres that defines the three-dimensional vehicle noise characteristics over a range of flight conditions. These source noise semi-spheres are built from acoustic flyover data by "de-propagating" the acoustic ground measurements to a location on a semi-sphere that has the vehicle position as its center. The accuracy of the source noise semi-sphere database is highly dependent on the quality of the flight test acoustic measurements, vehicle flight track measurements, vehicle orientation measurements along the flight track, vehicle operating state measurements, and measurement of the local meteorological conditions for a range of altitudes. Recent technological advances now allow for the accurate, yet relatively inexpensive measurement of not only the noise and the vehicle position, but also the vehicle fuselage orientation (roll, pitch, and heading) along the flight path. In addition, the development of accurate, low cost, on-board tracking systems using Differential GPS systems has allowed for low cost methods to provide significantly improved flight track guidance cues (Ref. 9) to the pilots. Accurate measurement of the vehicle position and its propulsor orientation relative to the ground microphone array is important to the development of accurate noise semi-spheres. Due to the complexity and expense of current rotor flapping measurement systems, the propulsor orientation is assumed to be equal to the vehicle fuselage orientation (roll, pitch, and heading). If vehicle fuselage orientation data are not available, then RNM estimates the orientation from the measured tracking data. RNM estimates the pitch and heading angles to be parallel to the flight track, and assumes the roll angle to be zero. The sensitivity of the semi-sphere levels to the estimated vehicle-orientation-method is not well established at this time. However, assessment of this sensitivity is needed to define accuracy requirements for flight test measurements, particularly those obtained to generate noise semi-spheres for use in RNM.

Two flight tests will be discussed in this paper. Both of these tests were conducted in the panhandle area of Florida, at a remote test range (Test Area C-72) of the Eglin Air Force Base. The first test was conducted in September 2003, and is referred to as the "Acoustic Week Flight Test", or "Eglin03". The U.S. Army's AFDD-JRPO and Aviation Applied Technology Directorate (AATD), along with the NASA LaRC were the primary participants in this test. The second test was conducted in October and November 2005, and is referred to as the "NASA Heavy Lift Rotorcraft Acoustic Flight Test", or "Eglin05". The NASA LaRC, AFDD-JRPO, and Sikorsky Aircraft were the primary participants in this second test. The primary purpose for both tests was to obtain benchmark rotorcraft acoustic databases for (1) validation of acoustic prediction programs such as RNM and (2) acquisition of a database of acoustic source noise characteristics to be used for low noise flight procedures development and for environmental impact assessments. This paper provides an overview of the RNM and a detailed description of the Acoustic Repropagation Technique that is used to build noise semi-spheres from measured acoustic flyover data. An overview of the Eglin03 and Eglin05 acoustic flight tests is provided, including the instrumentation systems, the test vehicles and the test matrix for each vehicle, the test procedures, and the data processing. Results using

the MD600N data acquired during the Eglin05 test are presented that show the effect of level flyover airspeed and the effect of descent angle on the RNM predicted ground noise levels. Finally, the sensitivity of the RNM predicted ground noise footprints to the vehicle-orientation-method (used while building the noise semi-spheres from measured data) is explored.

Rotorcraft Noise Model (RNM)

The Rotorcraft Noise Model (RNM) was initially created to (1) provide a tool to aid in the development and assessment of low noise terminal area operating procedures for rotorcraft and tiltrotors, and (2) improve rotorcraft community noise impact modeling capabilities. RNM is capable of providing information that can be imported into a Geographical Information System (GIS). The noise contours can then be overlaid to scale on a background map. This method is ideal for performing noise abatement studies, airport and vertiport noise impact evaluations, and land-use planning studies. Development of RNM began in the mid-1990s and continues with on-going and planned improvements and enhancements.

RNM is a simulation program that models sound propagation through the atmosphere and predicts various noise levels or noise metrics at receiver locations on flat ground or varying terrain (Ref. 10). RNM can perform these simulations for a single flight operation of a single vehicle, or for multiple flight operations for one or more vehicles. Detailed vehicle source noise characteristics, in the form of 3-dimensional sound semi-spheres, are required as input to RNM. As the vehicle "flies" along the prescribed flight trajectory, the source sound propagation is simulated and accumulated at receiver locations (single points of interest or multiple grid points). These sound signals at the receiver locations may then be analyzed to obtain single event footprints, integrated noise contours, metric time histories, or numerous other noise metrics of interest for either civil or military aspects of rotorcraft operations. RNM may also be used to generate spectral time history data over a ground mesh for the creation of single-event sound level animations.

The major computational and physical elements of the RNM are the sound propagation module and the input and output modules. As input, RNM requires source noise semi-spheres, vehicle flight track, flight profile orientation, and operating state. Vehicle operations are quantified along a set of user-defined, vectored flight tracks (Figure 1). The vehicle flight is simulated in a time-based domain along a prescribed flight track and the sound is analytically propagated through the atmosphere to the specified receiver locations. RNM currently accounts for spherical spreading, atmospheric absorption, ground reflection and attenuation, Doppler shifts, and the difference in phase between the direct and reflected rays. RNM allows for the prediction of noise over varying ground terrain using an implementation of the Geometrical Theory of Diffraction, including extensions for diffraction as developed by Rasmussen (Ref. 11). Modifications to include the effects of winds and temperature for a two-dimensional stratified atmosphere have been developed and implemented but have not been validated.

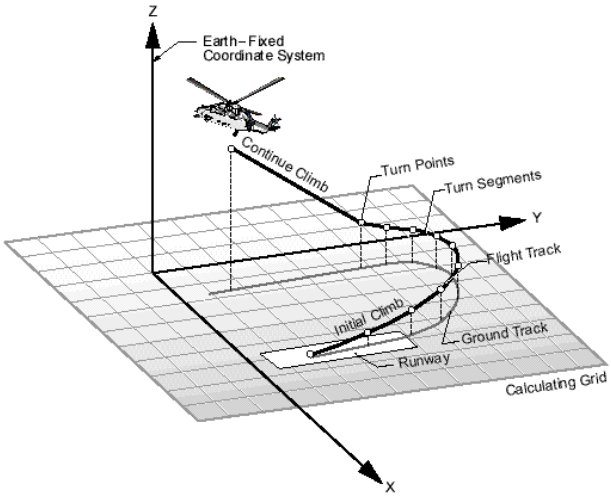

Figure 1. RNM single flight track definition.

Acoustic properties of the noise source(s) are defined in terms of source noise semi-spheres that may be obtained from theoretical predictions, wind tunnel experiments, flight test measurements, or a combination of the three. The sound semi-spheres may contain broadband data (source levels as a function of one-third octave band), narrowband data (amplitude only), or pure-tone data (in the form of specific frequency sound pressure levels and phase). Points on the semi-sphere are described in terms of a fixed radius and two spherical angles, θ and ϕ, representing the sphere azimuth and elevation angles. An example rotorcraft source noise semi-sphere is shown in Figure 2. θ is 0° at the nose and 180° at the tail while ϕ is -90° to the port, 0° below, and 90° at the starboard hub plane. When used in RNM, the source noise semi-sphere translates and rotates with the source vehicle trajectory and orientation. RNM will perform the atmospheric propagation for up to ten independently defined sound sources for a given vehicle. This is useful to independently define multiple noise sources for a single vehicle (*e.g.*, main rotor(s) noise, tail rotor noise, engine noise, *etc.*) or to

describe a single noise source as a combination of pure tone semi-spheres and a broadband semi-sphere. Each sound semi-sphere contains acoustic information for a single aircraft flight condition and each semi-sphere file contains a set of attributes that define the flight condition using three independent variables: airspeed, flight path angle, and nacelle pylon angle (for tiltrotor). For conventional helicopters, the nacelle pylon angle is fixed at 90 degrees.

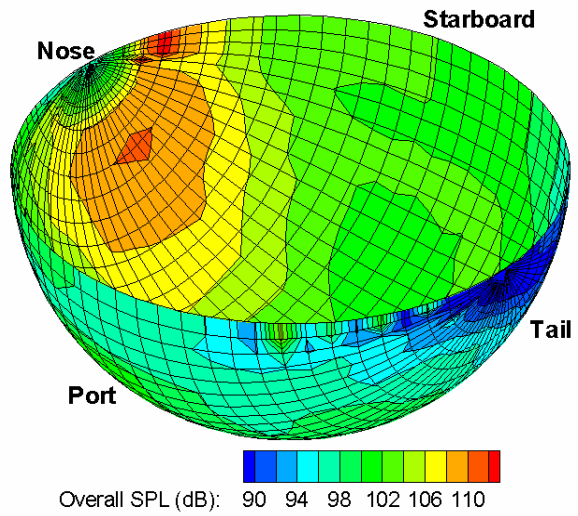

Figure 2. Example source noise semi-sphere.

Acoustic Repropagation Technique (ART)

The building of the source noise semi-spheres (such as the one shown in Figure 2) from test flight data is a two step process using version 5 of the RNM and the Acoustic Repropagation Technique (ART) computer codes (Refs. 12 & 13). The physics of the propagation from the source to the receiver is handled in RNM by calculating the effects of spherical spreading, atmospheric absorption, and ground reflections. The ART program uses the propagation effects along with the measured microphone data to assemble the semi-sphere.

The noise semi-sphere building process is shown graphically in Figure 3. The aircraft flies through a linear microphone array that is perpendicular to the ground track (projection of the flight track on the ground) at a constant operating condition as shown in Figure 3a. Noise spectra are computed from the measured acoustic pressure time histories at a selected time interval (typically every 0.5 seconds) over the duration of the flyover. Each noise spectrum is related to the aircraft position relative to each microphone (Figure 3b) thus providing noise levels as a function of the emission angles (Note: for clarity, the vertical portions of the microphone arrays are not shown in figures 3b and c). By freezing the aircraft at a point in space, these noise directivity data are projected onto the ground, as shown in Figure 3c, producing a detailed, high-resolution, effective ground noise contour that moves with the vehicle. The measured noise levels are then de-propagated to a semi-sphere of selected radius (Figure 3d and Figure 2). While the example shown in Figure 3 is for level flight, the same technique can also be used for steady-state ascending or descending flight. Since helicopter noise is significantly directional compared to fixed-wing aircraft, the measurement technique must capture these unique characteristics. Capturing this level of detail requires many more measurement locations than just the three measurement locations required for certification tests.

The propulsor (rotor) orientation along the flight track, relative to the ground microphone array, affects projection of the measured acoustic data to the noise semi-sphere. RNM/ART currently assumes that the vehicle fuselage orientation is the same as the propulsor orientation. The RNM/ART code allows the use of measured vehicle fuselage orientation data (roll, pitch, and heading angles). As an option, when these data are not available, the code will estimate the vehicle orientation based on the flight track data. When estimating the vehicle orientation angles, RNM/ART assumes that the vehicle roll angle is zero, and derives the heading and pitch angles from the trajectory of each flight track segment along the entire flight track. Depending on the directivity characteristics of the noise source, the orientation of the vehicle can be very important in generating accurate noise semi-spheres.

The goal of the noise semi-sphere building technique is to "populate" all of the semi-sphere grid points using the measured data. Figure 4a shows an overlay of the computed (from measured) data grid on the semi-sphere grid for the MD600N flying in level flight at 150 feet altitude and 90 knots airspeed through the microphone array. The closed black squares represent the points on the semi-sphere for each computed noise spectrum, while the open red squares represent the grid points of a semi-sphere with a typical 5° angular resolution. Note that the noise semi-sphere building technique does not always provide sufficient measured data to populate the noise semi-sphere all the way to the rotor tip-path-plane. For the level flyover, Figure 4a shows that measured data were acquired laterally up to the rotor tip-path plane ($\phi = 90°$ and $-90°$) except in the region near the tail of the vehicle ($\theta = 180°$). It should be noted that because the aircraft flyover altitude was 25 feet below the highest microphones on the cranes, data were measured above the rotor tip-path-plane where ϕ is greater than $\pm 90°$. To determine the

values on the semi-sphere grid from the values on the computed grid, the ART program provides a user selectable blend of Laplace and spline interpolation schemes. The user selects the range of computed grid points over which to interpolate; a larger range equates to the use of more measured points in the interpolation. This flexibility allows the building of noise semi-spheres from a sparsely measured set of data, but with a reduced fidelity.

An overlay of the computed spectra grid on the semi-sphere grid for the MD600N flying a 90 knot, 6 degree descent that passed over the microphone array at 250 feet altitude is shown in Figure 4b. In this case, a significant number of semi-sphere grid points lie outside the region where measured data was acquired, especially near the rotor tip-path-plane to the port side. In previous versions of ART, the region of the semi-sphere beyond which there is no data was populated by assuming that the levels are constant near the rotor tip-path plane. The level from the nearest angle below the rotor tip-path-plane for which data were measured was used to populate those grid points up to the rotor tip-path-plane. The results obtained using this assumption may or may not be acceptable. The questionable acceptability stems from the fact that the results will depend on many variables, including the angular distance over which the constant level is assumed, the vehicle noise directivity characteristics, and the vehicle operating condition. As a result, the current version of ART does not attempt to extrapolate to regions of the semi-sphere beyond which there is no measured data. To identify these regions, ART now assigns a value of $1x10^{35}$ to the spectrum for all parts of the semi-sphere where there is no measured data. This set value instructs RNM not to use that part of the semi-sphere when propagating the source to the ground.

ART has additional features that give the user flexibility over how the noise semi-sphere is built. The θ range, the ϕ range, the resolution of the noise semi-sphere, and the number of frequency bands that are de-propagated to each semi-sphere grid point are all user selectable. This flexibility enables a semi-sphere to be created when the measured data set consists of only a small number of measurement points. However, this will obviously affect the fidelity of the semi-sphere, and hence, will likely reduce the accuracy of any ground noise predictions made using this semi-sphere.

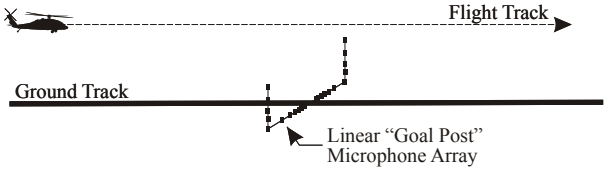

a) Source flyover of a linear microphone array.

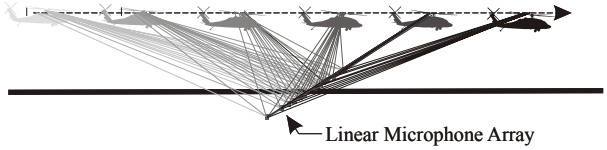

b) Acoustic data measured during flyover.

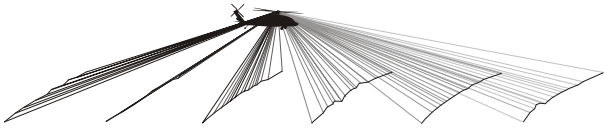

c) Single source location transformation.

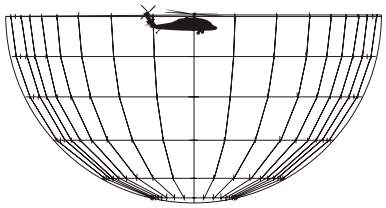

d) Source noise hemisphere.

Figure 3. Source noise measurement procedure.

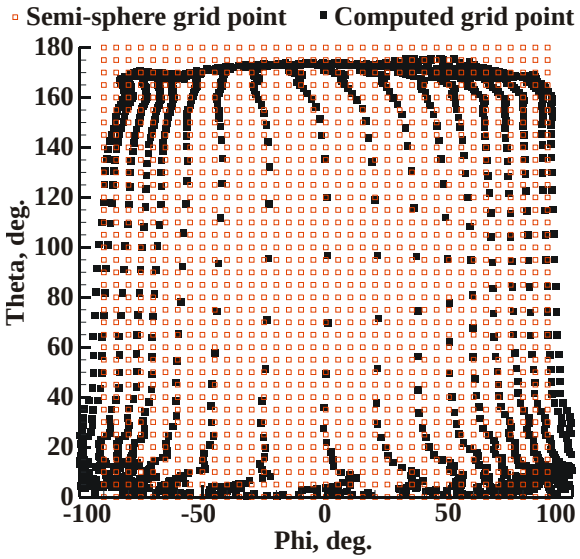

a) 90 knot level flyover at 150 feet altitude; MD600N.

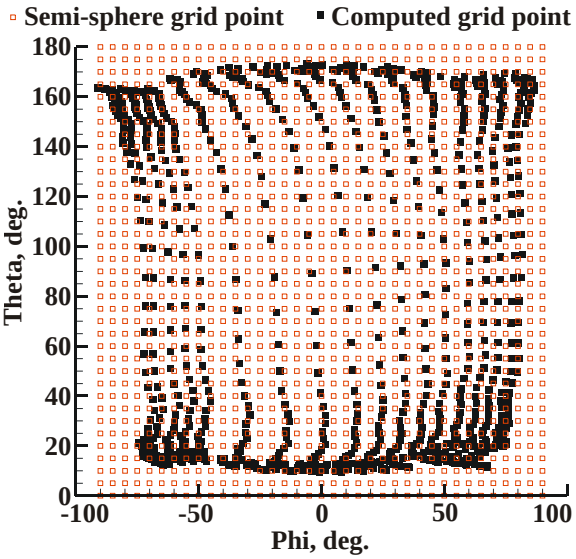

b) 90 knot 6° approach passing through microphone array at 250 feet altitude; MD600N.

Figure 4. Overlay of measurement data grid on a semi-sphere grid with 5° angular resolution.

Experimental Setup

Acoustic Instrumentation

NASA Langley's Digital Acoustic Measurement System (DAMS) was used to deploy a 30-microphone array during the Acoustic Week flight test program in 2003 (Eglin03). One-half inch pressure response condenser microphones fitted with grid caps and standard 4 inch wind screens were used. The DAMS microphone signals were low-pass filtered at 11,670 Hz and digitized at the microphone power supply box (25 kHz sample rate), transmitted via cables to a data van, multiplexed with time and test run information, and then recorded on magnetic media (Ref. 14). Three DAMS acoustic data vans were deployed, each containing a 10-microphone system. The microphone array for the Eglin03 test was specifically designed to measure a source noise semi-sphere for level flight conditions only. Due to an Acoustic Week emphasis on acoustic detection signatures, the microphone array setup shown in Figure 3a was modified to provide improved accuracy for the in-plane noise measurements forward of the rotorcraft, where initial acoustic detection typically occurs. The modified microphone array is shown in Figure 5. Figure 5a is a 3-dimensional sketch of the overall microphone layout, which consisted of a "goal-post" array and a "north-pole" array. The "goal-post" array was created by suspending four microphones from each of two cranes and deploying 12 microphones on ground boards between the two vertical arrays, as shown in Figure 5b. The distance between vertical arrays was 800 feet and the highest microphone in each vertical array was located 175 feet above ground level (AGL). The microphone positions were selected to provide approximately equal angular resolution for the acoustic measurements (up to and even slightly above the rotor plane) when the aircraft flew along the intended flight track between the vertical arrays at 150 feet altitude, as indicated by the red '+' sign in the figure. The "north-pole" microphone array was deployed to improve the fidelity of noise measurements directly in front of the vehicle. The vertical portion of the array was deployed on the flight track centerline, 5000 feet down range from the goal-post array. Six microphones were suspended from the north-pole crane at heights of 30, 60, 90, 120, 150, and 175 feet AGL and four microphones were deployed on ground boards along the flight track in front of the vertical array at distances of 0, 500, 1000 and 2000 feet (measured toward the goal-post array) from the base of the crane.

The microphone array deployed in the 2005 NASA Heavy Lift Rotorcraft Acoustic Flight Test (Eglin05) was similar to that shown in Figure 3a, with the exception that two microphones were located on each side of the array, outside of the vertical portions of the array. The 22-microphone array (Figure 6) was designed to measure source noise semi-spheres for level, ascending, and descending flight conditions (Figure 7). The 600 and 1200 foot sideline microphone positions were added to improve the sideline angular coverage for ascending and descending flight cases in which the

aircraft was at altitudes greatly in excess of 150 feet. Twenty microphone positions were supported using the DAMS while the two 1200 foot microphone positions were supported using the new NASA LaRC developed Wireless Acoustic Measurement System (WAMS). Similar to the DAMS, the WAMS utilized one-half inch pressure response condenser microphones fitted with grid caps and standard 4 inch wind screens and the microphone signals were digitized in the microphone power supply boxes. The WAMS digitizes at a 25 kHz sample rate, low-pass filters at 12.5 kHz, then records the data internally on a compact flash card. Improved analog to digital circuitry provides a greater signal to noise ratio and therefore a reduced noise floor compared to the DAMS. Data acquisition is initiated and terminated via an RF (Radio Frequency) link to a remote computer that can be located as far as 50 miles from the remote microphone box.

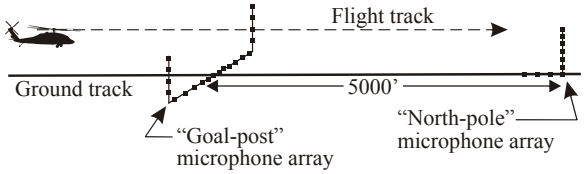

a) 3-dimensional sketch showing flight track.

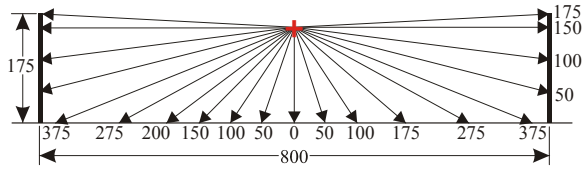

b) Goal-post array details.

Figure 5. Microphone array deployed during the Eglin03 flight test (dimensions in feet).

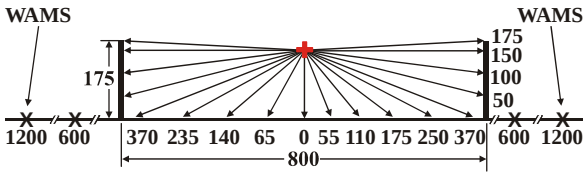

Figure 6. Microphone array deployed during the Eglin05 flight test (dimensions in feet).

Meteorological Instrumentation

A tethered weather balloon system was used to acquire weather profiles during each period of acoustic data acquisition. This system consisted of an electric winch-controlled, tethered helium-filled balloon, an instrument/telemetry pod, a ground-based receiver/data-controller, and a ground-based support computer. Profiles of temperature, relative humidity, wind speed, and wind direction were acquired up to 250-ft altitude continuously during all periods of acoustic data acquisition. The weather balloon was continuously cycled up and down at a rate of approximately 1 foot per second. An example of the weather data profiles for a typical test period is presented in Figure 8. Weather conditions can dramatically effect acoustic propagation, especially over long distances. The weather data can be used as input to the propagation module within RNM/ART, or simply to provide information to aid in the interpretation of any anomalies resulting from the acoustic measurements.

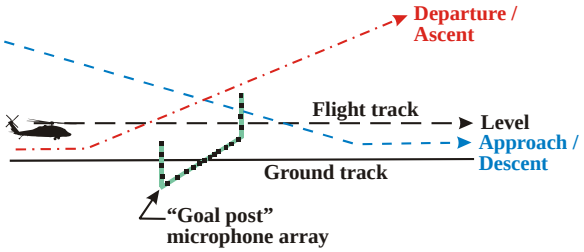

Figure 7. Flight track profiles flown during the Eglin05 flight test.

Test Aircraft

Nine vehicles were tested during the Eglin03 test program and three vehicles were tested during the Eglin05 test program. Table 1 provides a list of the vehicles tested, the date(s) that each vehicle was tested, and the organizations that were instrumental in securing participation of the vehicle.

Tracking, Guidance, and Vehicle Fuselage Orientation Instrumentation

Accurate vehicle position data during the acoustic measurements are essential to the generation of high-quality noise semi-spheres. Vehicle position data were acquired by six different organizations during these test programs. Table 2 lists each organization, the vehicles for which they were responsible, and whether the data were differentially corrected. Differential corrections generally improve position data accuracy from several meters to less than a meter.

The ability of the pilot to accurately fly the desired flight track is also important to the quality of the noise semi-spheres. For many of the test vehicles, the only lateral guidance cues were provided by white target cloths staked to the ground at regular intervals along the ground track centerline, while the only vertical guidance cues were provided by the standard cockpit pressure altimeter. Improved run quality was realized for a number of the test aircraft through the use of DGPS based flight track guidance systems. A guidance system developed by

Boeing-Mesa under contract to NASA LaRC was used on four of the vehicles while a Sikorsky developed system was used on the S-92A, as indicated in Table 2. These systems compared the real-time DGPS vehicle position data against desired vehicle position data and used the difference to drive a standard course and glide slope deviation indicator (CDI/GDI) mounted on the instrument panel. A comparison of flight tracks flown using the two different guidance methods showed dramatic improvements in flight track accuracy and repeatability with the cockpit guidance cues (Ref. 9). Unfortunately, resource limitations and/or flight safety requirements did not allow for installation of a guidance system in all of the test vehicles.

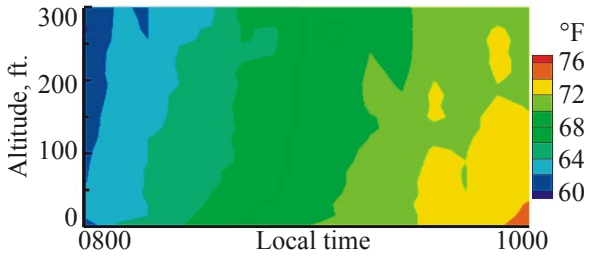

a) Temperature.

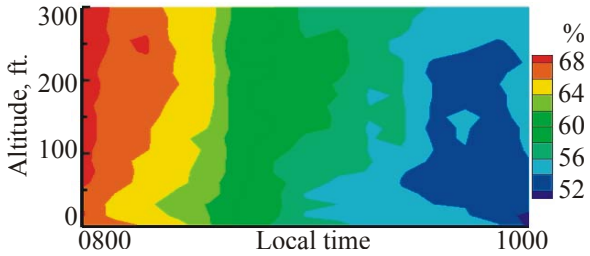

b) Humidity.

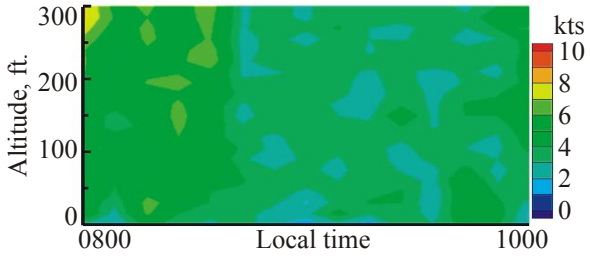

c) Wind speed.

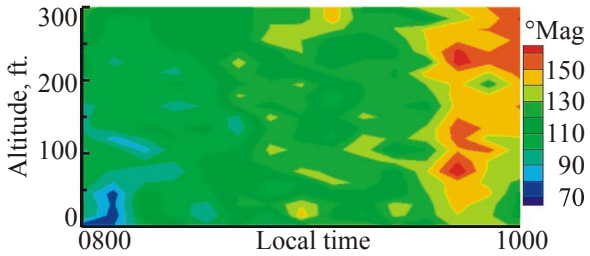

d) Wind direction.

Figure 8. Sample weather profile acquired during a MD600N test period from the Eglin05 test.

Table 1. Test vehicles.

Date Tested	Vehicle	Providing Organization
9/8/03	Bell 206	Chicken Little
9/10/03	AH-64A	Ft. Rucker, Lead The Fleet, Chicken Little
9/11/03	K-MAX	LaRC/DARPA, Kaman, Northrop-Grumman
9/12/03	Schweizer 333 (FireScout prototype 2)	LaRC/DARPA, Schweizer, Northrop-Grumman
9/15/03	Aerostar UAV	NAVAIR
9/16/03	Bo105	LaRC/DARPA, Boeing-Mesa
9/17/03	UH-60L	Ft. Rucker, Lead The Fleet, Chicken Little
9/18/03	MD520N	LaRC/DARPA, Boeing-Mesa
9/19/03	TH-57	Wyle Laboratories
10/25, 26, 27 & 28/05	MD600N	LaRC/DARPA, Boeing-Mesa
11/3, 4 & 7/05	MH-53E	LaRC, NAVAIR
11/14, 15 & 18/05	S92A	Sikorsky Aircraft

During the Eglin05 test the NASA/Boeing-Mesa DGPS tracking and guidance system was modified to include measurement of vehicle fuselage orientation information. These modifications provided accurate measurement of the vehicle roll, pitch, and heading attitudes and rates. These data were recorded along with the vehicle position data.

Test Matrixes

During the Eglin03 test, flight time for each vehicle was limited to approximately 2 hours, which equates to about 20 runs. Due to the limited number of runs and the emphasis on aural detection, only level flyovers were conducted. Data were collected for level flyovers at 150 and 250 feet altitude and velocities of 60, 80, 100, and 120 knots or Vmax, as shown in Table 3. The maximum airspeed tested (Vmax) was vehicle dependent. For example, if the vehicle could achieve at least 120 knots, then 120 knots was the maximum airspeed tested. If a vehicle was incapable of reaching 120 knots, then the maximum airspeed tested was the maximum airspeed that vehicle was capable of flying. The 150-foot

altitude cases were the primary runs because this flight altitude allowed for the measurement of spherical angles, ϕ, to the vehicle port and starboard sides that were slightly above the rotor tip-path-plane. The 250-foot flyovers were flown to assess the effect of altitude, and hence the angular (θ) resolution (Ref. 15) on the noise semi-spheres as a result of the change in altitude. Multiple runs at each flight condition were acquired to improve the statistical confidence in the measured data.

Table 2. Organizational responsibilities for providing vehicle position measurements.

Organization	Vehicle(s)	Differential GPS
Chicken Little	Bell 206	Yes
Ft. Rucker, Lead The Fleet	AH-64A, UH-60L	No
LaRC, Boeing-Mesa	K-Max, Bo105*, MD520N*, MD600N*, MH-53E*	Yes
Northrop-Grumman	Schweizer333	Yes
NAVAIR	Aerostar	No
Sikorsky Aircraft	S92A**	Yes

* Cockpit guidance cues provided by LaRC.
** Cockpit guidance cues provided by Sikorsky.

Table 3. Test matrix indicating number of runs at each condition, for all vehicles for Eglin03 test.

Altitude, ft. / Velocity, kts.	60	80	100	120 / Vmax
150	2	3	3	4
250	2	3	3	

For the Eglin05 test, emphasis was placed on measuring the source noise for a wide variation of flight conditions for a fewer number of aircraft. The details of the test matrix were slightly different for each vehicle. Data were obtained for steady-state level and approach flight conditions for the MD600N, MH-53E, and S-92A, as indicated in Tables 4, 5, and 6, respectively. In addition, data were acquired for hover at 150 foot altitude, for steady-state take-offs at several airspeed / climb rate combinations, and for a number of maneuvers (*e.g.,* right and left turns, popup/pushovers, and roll doublets). The level flight condition marked by an asterisk (*) indicates a flight condition that was repeated frequently and is referred to as a "housekeeping run". Attempts were made to repeat the housekeeping runs at the beginning and end of each test period, to provide a measure of data variability.

Table 4. Level flight and approach test matrix for the MD600N indicating number of runs at each condition from Eglin05 test.

Decent angle, deg. / Velocity, kts.	0	3	6	9	12
50	2	2	2	1	1
70	4	4	4	4	
90	4	4	3	4	
110	12*				
125	4				

Table 5. Level flight and approach test matrix for the MH-53E indicating number of runs at each condition from Eglin05 test.

Decent angle, deg. / Velocity, kts.	0	3	6	9	12
40				2	
60	2	3	3	2	2
80	2	4	3	2	
100	7*	3	3		
120	3	3			
140	3				
Vmax (165 – 170)	3				

Table 6. Level flight and approach test matrix for the S-92A indicating number of runs at each condition from Eglin05 test.

a) 105% RPM

Decent angle, deg. / Velocity, kts.	0	3	6	9	12
50			6	4	
60			5	5	
80			5	4	
120	4				
130	2*				

a) 95% RPM

Decent angle, deg. / Velocity, kts.	0	3	6	9	12
50					
60					
80			4		
120					
130	3*				

Test Procedures

A simple race track flight pattern was used during both the Eglin03 and Eglin05 flight tests. The aircraft approached the goal-post microphone array from a distance great enough to allow the pilot to achieve a steady-state flight condition on the prescribed flight path at the prescribed airspeed prior

to the initialization of acoustic data acquisition. The objective was to fly through the goal-post microphone array while maintaining the steady state flight condition for a prescribed distance before and after the microphone array in order to capture as much of the noise semi-sphere as possible. For example, during the level flight runs, steady state conditions were held for a total distance of about 8000 feet, or 4000 feet before to 4000 feet past the goal-post array. A run, and data acquisition for the run, was considered complete when the pilot terminated the steady state flight condition. Figure 9 is a photo showing the MH-53E flying through the goal-post microphone array during the Eglin05 test.

Figure 9. Photo of MH-53E flying through the goal-post microphone array.

During the Eglin05 test, approach profiles were flown for descent angles ranging from 3° to 12°, as shown in Figure 10 (note: outlying microphones are not shown in the figure). For all descent angles, the target altitude, h, over the microphone array remained the same for each vehicle: h = 250 feet for the MD600N and h = 300 feet for the MH-53E and S-92A. This increased altitude over the microphone array compared to the level flights was done to allow for measurement of a greater range of the aft portion of the noise semi-sphere prior to pulling out of the steady state descent flight condition. Acoustic data acquisition was initiated 5000 feet before the microphone array and terminated when the pilot pulled out of the descent. For safety reasons the pull-out was initiated at the pilot's discretion, and was typically between 50 and 100 feet AGL.

Take-off profiles were flown for a range of climb rates ranging from 500 to 2300 feet per minute. The goal was to approach the microphone array at a prescribed altitude (50 feet) and airspeed (50 to 120 knot range), then pull into a steady-state climb with the target of passing over the microphone array at an altitude of h feet, where h = 250 feet for the MD600N and h = 300 feet for the MH-53E and S-92A, as shown in Figure 11. Acoustic data acquisition began prior to pulling up into the climb and was terminated when the aircraft was approximately 5000 feet beyond the microphone array.

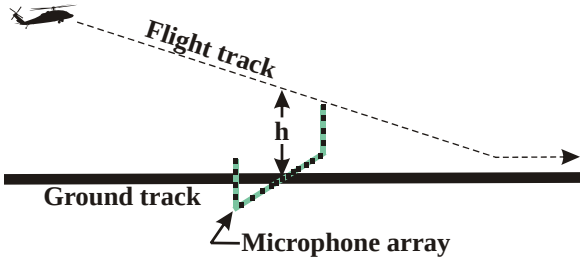

Figure 10. Sketch of approach profile.

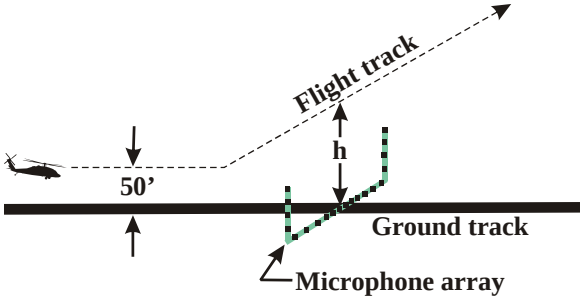

Figure 11. Sketch of take-off profile.

Results and Discussion

Data Processing

All acoustic results presented in this paper were obtained from measured pressure time history and spectral data and from one-third octave band source noise semi-spheres. The noise semi-spheres were created with the RNM/ART version 5 using measured roll, pitch, and heading angle data, flight track data, and acoustic data. All narrowband analyses used the average of five 4096-point FFTs with a Hamming window and 50% overlap applied, resulting in 0.4915-second data blocks. These averaged narrowband spectra were computed every 0.5 seconds for each microphone for the duration of each flyover. The narrowband spectra were then integrated to obtain one-third octave band spectra. The RNM/ART was used to generate one-third octave band source noise semi-spheres using the on-third octave band spectra that were computed from the measured data. Ground noise footprints were then predicted with RNM, using the source noise semi-spheres (created from measured data), for specific flight track and vehicle operating conditions.

The one-third octave band spectra on the predicted ground footprint were integrated to obtain Overall Sound Pressure Levels (OASPL), or were optionally filtered and integrated to obtain A-weighted Overall Sound Pressure Levels (L_A or dBA). Sound Exposure Levels (SEL) were obtained by integrating the L_A over the duration of the flyover for which the levels were within 10 dBA of the peak level. Unless otherwise specified, all of the results presented were generated using RNM and the MD600N noise semi-spheres obtained during the Eglin05 flight test. The XV-15 results presented were also processed as discussed above. The following results demonstrate some of the capabilities of the RNM.

Data Repeatability

To assess the variability of the data during a specific test day and over multiple test days, the 110 knot level flyover at 150-feet altitude was repeated frequently. This "housekeeping" condition was typically, as a minimum, the first and last run of each test flight. For the MD600N, seven housekeeping runs were conducted during two test days. To show the repeatability of the data acquired during these two test days, RNM was run seven times, each time using as input a source noise semi-sphere generated from each of the seven housekeeping runs. Figure 12 shows the variation of SEL for sideline distances between ±3000 feet of the flight track centerline. The figure shows that, as one would expect, the maximum sound exposure levels are at the flight track centerline and decrease rapidly with increasing sideline distance. The SEL variation between housekeeping runs for all sideline distances is approximately ±0.5 dBA. It is felt that this variability is due to variations in the wind conditions that required changes in the control inputs and vehicle operating condition to maintain the desired flight path. To minimize the effect of winds on the measured acoustic data, testing was not conducted if ground winds exceeded 10 knots or when the crosswind component exceeded 10 knots at any altitude that the vehicle was required to operate in during acquisition of primary acoustic data. Without the flight track guidance system, the variability would likely be much greater given the flight track variability shown in reference 9.

Effect of Airspeed for Level Flyovers

The variation of the SEL metric with sideline distance for five airspeeds ranging from 50 to 125 knots is presented in Figure 13. The slowest airspeed (50 knots) produced the highest levels on the flight track centerline while the highest airspeed (125 knots) produced the highest levels at sideline distances from about 600 to 3000 feet. Levels at the centerline decreased with airspeed from a maximum of 93.7 dBA at 50 knots, to a minimum of 87.1 dBA at 110 knots, and then increased slightly to 88.8 dBA at 125 knots. At 3000 feet to either sideline the levels were about 30 dBA lower than directly under the vehicle, varying from about 59 to 62 dBA. The 50 and 125 knot runs produced the highest levels and the 70 and 90 knot runs produced the lowest levels.

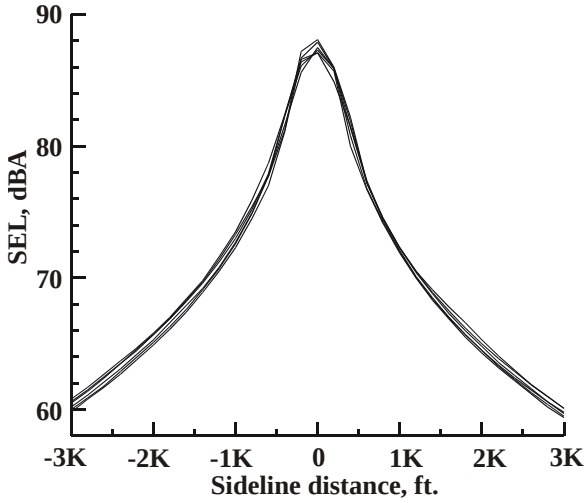

Figure 12. Variability of RNM predicted sound exposure levels for housekeeping runs; level flyovers at 110 knots; MD600N.

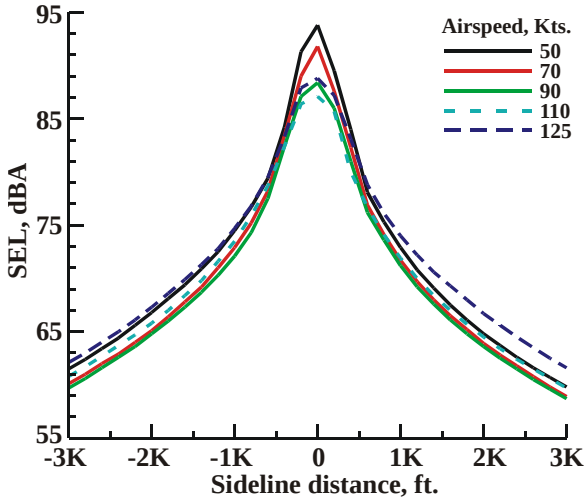

Figure 13. Variation of SEL with sideline distance for airspeeds of 50 to 125 knots; MD600N.

The SEL metric provides a measure of annoyance by considering a combination of the duration of exposure and the noise level. By examining the maximum A-weighted overall sound pressure level, or dBAmax, that occurs during a

flyover, the effect of duration is eliminated. Figure 14 presents the dBAmax as a function of the sideline distance for each of the five flyovers presented in Figure 13. Again, the 50 knot flyover produced the highest level on the flight track centerline while the 125 knot case clearly produced the highest levels for all sideline distances greater than about 500 feet. At the centerline, the levels decrease with airspeed from a maximum of 90.0 dBAmax at 50 knots to a minimum of 85.3 dBAmax at 90 knots, and then increase with airspeed to 87.4 dBAmax at 125 knots. At 3000 feet to either sideline, the levels were about 40 dBAmax lower than at the centerline, varying from about 44 to 49 dBAmax. The 125 knot run produced the highest sideline levels, while the 50, 70, and 90 knot runs produced approximately equal levels at the minimum values.

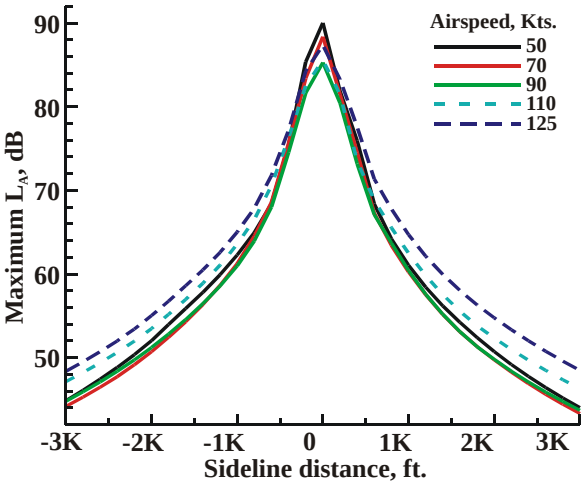

Figure 14. Variation of the maximum dBA level with sideline distance for airspeeds of 50 to 125 knots; MD600N

To investigate why the slowest flyover speed (50 knots) produces the highest A-weighted levels on the flight track centerline, the one-third-octave band spectra for the maximum *measured* L_A at the centerline microphone position were examined. These peak levels occurred just prior to the overhead position, which means that the observer location was below, and just out front of, the vehicle. Figure 15 presents the centerline A-weighted, one-third octave band spectra for the 50 and 90 knot runs shown in Figure 14. The fundamental blade passage frequency occurs in the 50 Hz band at a level of about 50 dB for both runs. The first and second harmonics are also nearly equal for these two runs. The primary difference between these runs is the elevated levels for the 50 knot run in the frequency range of about 500 to 5000 Hz. The maximum difference is about 6 dBA at about 1500 Hz. The narrowband spectra were examined to determine if this could be due to the NOTAR fan, which has a fundamental blade passage frequency of 1167 Hz and a thruster that is directed downward. Noise from the anti-torque thruster was not evident in the noise spectra until just after the vehicle passed overhead, when the observer position was below and behind the vehicle. The elevated levels from 500 to 5000 Hz are broadband in nature and are believed to be due to Blade Wake Interaction (BWI) noise. At the slower speeds the rotor plane is nearly parallel to the relative wind and the rotor blades are interacting with the turbulent (non-deterministic) portions of the wake from preceding blades. As the aircraft speed is increased the rotor pitches down with respect to the relative wind and the entire rotor wake tends to move below the rotor plane. This conclusion is supported by the findings in reference 16 (Figure 2 in the reference).

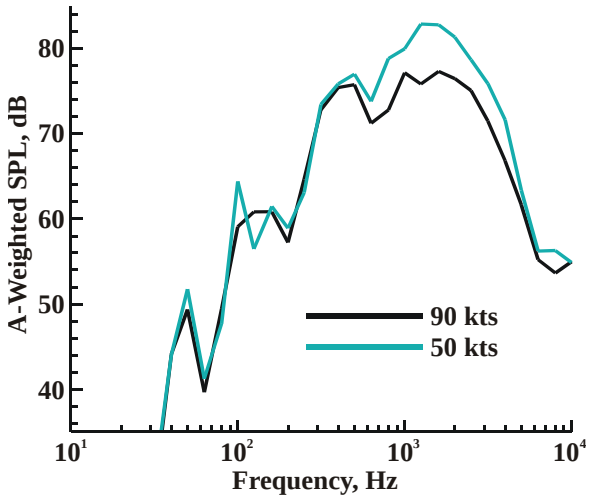

Figure 15. *Measured* centerline A-weighted one-third-octave band spectra for maximum L_A; MD600N.

Effect of Descent Angle at Constant Airspeed

In this section the effect of descent angle on the MD600N noise footprint is examined for the constant airspeed of 90 knots. Figure 16 shows the RNM predicted SEL footprint for a 6° approach. An ideal flight path was used in the RNM input deck. That is, the sideline distance is always zero (Y = 0), and altitude, Z, increases at a 6° angle from the ground intercept point (X = 0). The simulated approach begins with the aircraft located 15,000 feet up-range of the landing point (X = -15,000 feet) and continues to the ground intercept point. The footprint extends from 1000 feet to 8000 feet up-range of the intended landing point (X = -1000 to -8000 feet) and spans to 3000 feet to either side of the flight track centerline (Y = 0). The aircraft is moving from left to the right

in the figure, along the flight track centerline, with an altitude profile that would intersect the ground (Z = 0) at the point X = Y = 0. The predicted SEL levels varied from 62 to 97 dBA. Maximum levels occurred beneath the aircraft, just slightly to the starboard side of the flight track (advancing rotor side), and decreased with increasing sideline distance for all up-range distances. Along the flight track the levels increased from 86 dBA at 8000 feet up-range to 96 dBA at 1000 feet up-range. At the 3000 foot sideline distances to either side of the aircraft the levels varied from 63 dBA to 69 dBA.

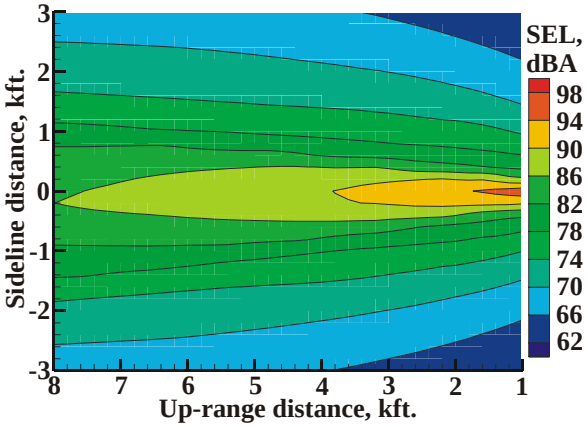

Figure 16. SEL footprint for 6° approach profile; MD600N.

The SEL footprint for the 3° approach profile is presented in Figure 17. Compared to the 6° approach, noise levels decrease more rapidly with increasing sideline distance, but at about the same rate along the flight track with increasing up-range distance. Along the flight track the levels increase from 86 dBA at 8000 feet up-range to 95 dBA at 1000 feet up-range. The sideline noise levels vary from 57 dBA to 65 dBA. Figure 18 presents a footprint of the difference between the 3° and 6° approaches. A positive value indicates that the 3° approach is louder than the 6° approach. The figure shows that the 3° approach is quieter than the 6° approach throughout the entire footprint with the exception of a small area along the flight track between about 7000 and 8000 feet up-range, where the levels are essentially equal. Noise reductions along the flight track varied from about 0 dBA to 1.5 dBA, while noise reductions along the sidelines varied from about 4 dBA to 7 dBA. The 3° approach appears to be a quieter operating condition than the 6° approach with the greatest noise reductions occurring at the larger sideline distances. In general, the noise reductions increase with increasing sideline distance and with decreasing up-range distance. This is due to a combination of the difference in source-to-receiver propagation distances dictated by the change in approach angle and the source directivity characteristics of the vehicle. When comparing a 3° approach profile to a 6° approach profile, it should be noted that the difference in the source-to-receiver propagation distance is greatest directly beneath the aircraft and decreases dramatically with increasing sideline and up-range distances. For example, directly beneath the aircraft the source-to-receiver distance for the 3° approach is precisely half that for the 6° approach for all up-range distances. However, at 8000 feet up-range and 3000 feet to the sideline the source-to-receiver propagation distance for the 3° approach is only about 3% less than that for the 6° approach and at 6000 feet to the sideline the difference reduces to 0.7%.

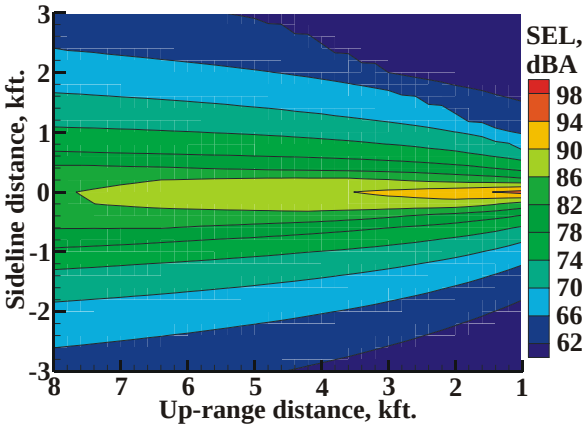

Figure 17. SEL footprint for 3° approach profile; MD600N.

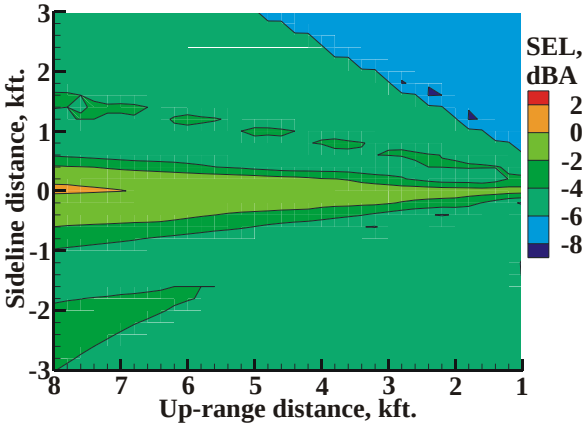

Figure 18. SEL footprint of difference between 3° and 6° approach profiles; MD600N.

The SEL footprint for the 9° approach profile is presented in Figure 19. Compared to the 6° approach, the effect is nearly opposite that seen for the 3° comparison. Levels decrease less rapidly with increasing sideline distance and decrease more rapidly along the flight track with increasing up-range distance. Along the flight track the levels

increase from 81 dBA at 8000 feet up-range to 92 dBA at 1000 feet up-range. The sideline levels vary from 62 dBA to 70 dBA. Figure 20 presents a footprint of the difference between the 9° and 6° approaches, with a positive value indicating that the 9° approach is louder than the 6° approach. Throughout much of the footprint the 9° approach is slightly louder (0 to 2 dBA) than the 6° approach, Along the flight track, where the difference in propagation distance is the greatest, the 9° approach has significant noise reductions of between 4 and 5 dBA. The noise reductions decrease with increasing sideline distance, as the propagation distances become about equal for the 6° and 9° approaches. In general, the 9° approach appears to be a slightly louder operating condition than the 6° approach, due to the change in flight condition. However, lower levels are obtained near the flight track due to the increased source-to-receiver propagation distance caused by the change to a steeper approach angle.

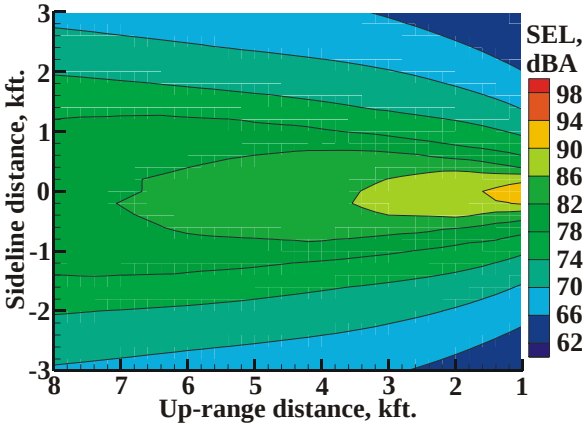

Figure 19. SEL footprint for 9° approach profile; MD600N.

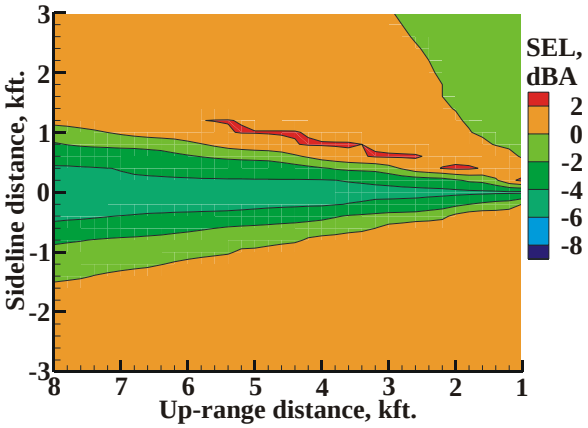

Figure 20. SEL footprint of difference between 9° and 6° approach profiles; MD600N.

Noise Prediction Sensitivity to Vehicle Orientation angles.

In this section the sensitivity of the RNM predicted noise footprints to the vehicle orientation angles used by RNM/ART in the creation of the source noise semi-spheres is investigated. When creating a source noise semi-sphere using measured acoustic flyover data, the user has the option to input measured vehicle roll, pitch, and heading data or to require RNM/ART to estimate these values from the vehicle tracking data as described in the ART section earlier in this paper. The vast majority of flyover acoustic data that have been collected for the creation of RNM source noise semi-spheres have been obtained without the measurement of vehicle roll, pitch, and heading information because of the additional level of complexity and significant expense that this measurement capability can impose on a flight test. Therefore, most source noise semi-spheres that are available for use with RNM were created using the option that requires RNM/ART to predict the vehicle orientation angles. Vehicle roll, pitch, and heading angles were measured during the Eglin05 flight test and during a XV-15 noise test conducted by a NASA / Army / Bell Helicopter team in 1995 (Ref. 5).

Figure 21 presents the top view of a L_A semi-sphere for the MD600N that was created by RNM/ART using the measured roll, pitch, and heading data. Note that a compression of the noise level contours that are high up on the semi-sphere is inherent to this top view perspective. Also, the bright red areas around the perimeter of the semi-sphere indicate the areas for which there are no acoustic data available. The flight condition is a 6° approach at 90 knots and the contour interval is 2 dBA. This is the noise semi-sphere that was used by RNM to predict the SEL footprint shown in Figure 16. Though this is an operating condition that would typically contain some Blade Vortex Interaction (BVI) noise, which is a very directional noise source, this semi-sphere appears to have very benign noise directivity characteristics. In fact, examination of measured pressure time history data for all approach conditions (airspeeds and descent angles) obtained for the MD600N showed that any BVI events are suppressed, if they exist at all. This is not surprising since the MD600N has a lightly loaded, 6-bladed main rotor system. The lack of a tail rotor likely also contributes to the benign character of the noise semi-sphere. This noise semi-sphere was then used in RNM to predict the SEL ground footprint for an ideal 6° approach at 90 knots airspeed (Figure 16). In addition, RNM was executed again to predict the SEL ground footprint for an identical approach,

however, this time using a noise semi-sphere that was built using the RNM/ART estimated pitch and heading angles (roll is assumed zero) with the same measured acoustic and flight track data. The difference between these two RNM predicted footprints is presented in Figure 22. The figure shows that the ΔSPL was always between ±1 dBA. This is not surprising for this vehicle given the relatively benign nature of the directivity characteristics of the noise semi-sphere for changes in roll, pitch, and heading that were examined.

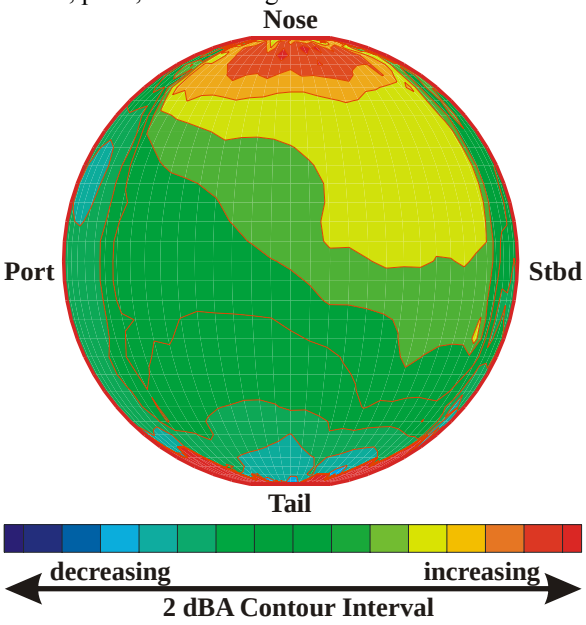

Figure 21. L_A semi-sphere created using measured vehicle fuselage orientation data; MD600N at 90 knots, 6° approach.

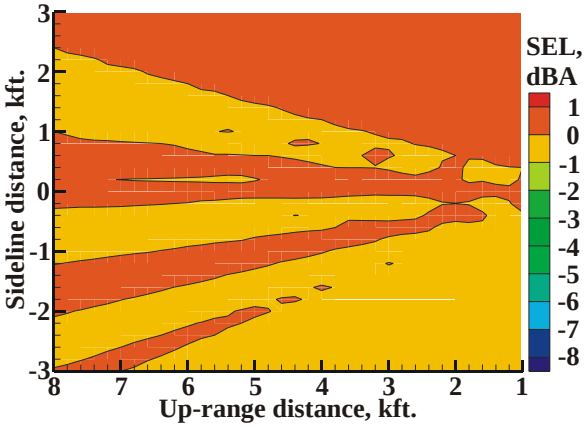

Figure 22. Delta SEL footprint showing the noise variation effect from using measured versus estimated vehicle fuselage orientation in the source noise semi-sphere creation process (RNM/ART); MD600N at 90 knots, 6° approach.

To examine the effect of the semi-sphere development procedure for a vehicle with known intense BVI events and complex directivity characteristics, noise semi-spheres for the XV-15 tiltrotor aircraft operating at 110 knots, 80° nacelle angle, on a 6° approach profile were created using the measured and RNM/ART estimated vehicle orientation techniques. Figure 23 shows the L_A semi-sphere created using the measured roll, pitch, and heading data. Compared to Figure 21, the complexity of the noise directivity characteristics for this semi-sphere is greatly increased. Figure 24 shows the XV-15 ΔSPL footprint, just as was presented for the MD600N in Figure22. This time,

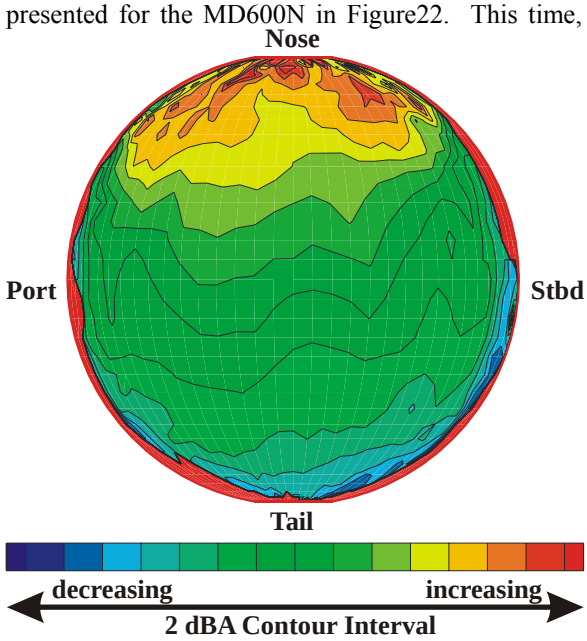

Figure 23. L_A semi-sphere created using measured vehicle fuselage orientation data; XV-15 at 110 knots, 6° approach, 80° nacelle angle.

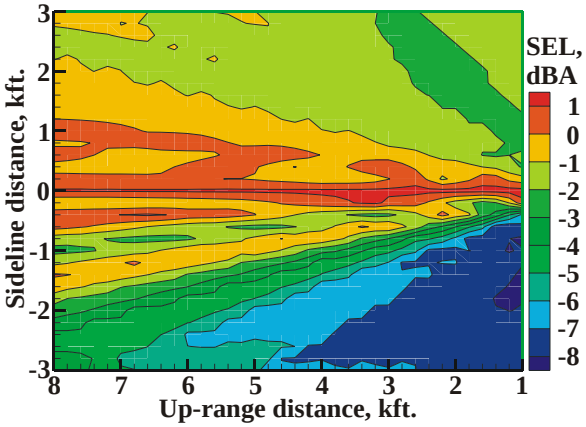

Figure 24. Delta SEL footprint showing the noise variation effect from using measured versus estimated vehicle fuselage orientation in the source noise semi-sphere creation process (RNM/ART); XV-15 at 110 knots, 6° approach, 80° nacelle angle.

in the RNM predicted footprints due to the use of measured vehicle fuselage orientation angles rather than the standard RNM/ART estimation method in the noise semi-sphere creation process. For this vehicle and flight condition, the dominant source for the noise footprint differences was the pitch angle.

These figures indicate that the sensitivity of the noise semi-spheres to the vehicle-orientation-method used in the RNM/ART prediction process, and hence the predicted noise footprints, can be significant and appears to be highly dependent on the vehicle design and flight condition. Typically the most prominent noise source is the rotor. The vehicle fuselage orientation is used in RNM/ART to define the position of the rotor. The development of a portable tracking and guidance system by Boeing-Mesa, under contract to NASA LaRC, and the recent incorporation of accurate roll, pitch, and heading sensors into the system, has just now made measurement of the vehicle fuselage orientation relatively simple and inexpensive. However, to more accurately define the rotor state in the RNM/ART model, flight measurements need to include a direct measurement of rotor tip-path-plane orientation with respect to the ground microphone array. This requires measurement of the rotor flapping angles in addition to the vehicle fuselage orientation. Measurement of rotor flapping angles is currently difficult and expensive, and is therefore not practical for most acoustic flight test opportunities.

Intuitively, one would think that noise semi-spheres and footprints predicted using measured vehicle roll, pitch, and heading data would be more accurate than the standard RNM/ART method of using pitch and heading angle estimates derived from the flight track data (with roll assumed zero). Though a rotor must flap in order to trim the vehicle, a rotor design goal is to minimize rotor flapping due to the loads and vibrations that it introduces into the rotor hub. Therefore, the assumption that the rotor tip-path-plane is the same as the vehicle fuselage orientation may be a very reasonable assumption for many flight conditions. The potentially high sensitivity of the predicted noise footprints to the vehicle pitch angle that has been shown in this study points out the need to modify RNM/ART to account for the rotor mast pre-tilt when using the measured vehicle attitude data. Rotor mast pre-tilt is a forward mast tilt (typically a few degrees) that is designed into most rotorcraft to provide a forward thrust vector from the main rotor with a reduced nose-down body pitch angle. This modification will be included in the next version of RNM/ART. Rotor mast pre-tilt was not accounted for in the noise semi-spheres used in this study. The issue of which of the current RNM/ART semi-sphere prediction methods produces the most accurate noise footprint predictions has not been addressed here, but the sensitivity of the footprint prediction was demonstrated. The two cases presented tend to the extremes of benign and complex directivity characteristics. The complexity of the directivity characteristics for most rotorcraft will likely fall somewhere between these two cases.

Conclusions

Two acoustic flight tests were conducted at a remote test range of the Eglin Air Force Base, the first in 2003 and the second in 2005. A benchmark acoustic flight database of source noise semi-spheres was created and is available for acoustic code validation, low noise flight procedures development and environmental impact assessments. An overview of the Rotor Noise Model (RNM) and a detailed description of the Acoustic Repropagation Technique (ART) used to build the source noise semi-spheres (from measured acoustic flyover data) required as input to RNM was presented.

Vehicle orientation along the flight path is required by RNM/ART to create the noise semi-spheres and for ground footprint predictions. An initial examination of the RNM prediction sensitivity to the propulsor orientation estimation method was presented. RNM predictions were found to be most sensitive for vehicle/flight condition combinations that exhibited strong and highly directional noise directivity characteristics.

RNM predictions were produced using source noise semi-spheres created by ART for the MD600N. A range of airspeeds and approach angles were examined. The following noise trends were found.

1. For the level flight conditions, the highest noise levels along the flight track centerline were obtained at the slowest airspeed flyover condition of 50 knots.
2. For the approach conditions measured (3°, 6° and 9°), the 9° approach was the quietest condition along the flight track centerline, with noise reductions of as much as 6 dBA compared to the 6° approach. However, off centerline the 9° approach showed elevated noise levels over much of the noise footprint.
3. The 3° approach was quietest for all areas off centerline, with average noise reductions of 4 to 6 dBA compared to the 6° approach condition.

References

1. Janakiram, R. D., O'Connell, J. M., Fredrickson, D. E., Conner, D. A. and Rutledge, C. K., "Development and Demonstration of Noise Abatement Approach Flight Operations for A Light Twin-engine Helicopter – MD Explorer," AHS Technical Specialists Meeting For Rotorcraft Acoustics and Aerodynamics, October 1997.

2. Jacobs, E. W., O'Connell, J. M., Conner, D. A., Rutledge, C. K., Wilson, M. R., Shigemoto, F., Chen, R., Fleming, G. G., "Acoustic Flight Testing of A Boeing MD Explorer and a Sikorsky S-76B Using a Large Area Microphone Array," AHS Technical Specialists Meeting For Rotorcraft Acoustics and Aerodynamics, October 1997.

3. Speigel, P., Buchholz, H., Pott-Pollenske, M., "Highly Instrumented BO105 and EC135-FHS Aeroacoustic Flight Tests Including Maneuver Flights," AHS 61st Annual Forum, Grapevine, TX, June 2005.

4. Yin, J., Spiegel, P., Buchholz, H., "Towards Noise Abatement Flight Procedure Design: DLR Rotorcraft Noise Ground Footprints Model and its Validation," 30th European Rotorcraft Forum, Marseilles, France, September 2004.

5. Conner, D. A., Edwards, D. B., Decker, W. A., Marcolini, M. A., Klein, P. D., "NASA/Army/Bell XV-15 Tiltrotor Low Noise Terminal Area Operations Flight Research Program," Journal of the American Helicopter Society, Volume 47, Number 4, October 2002, pp 219-232.

6. Munt, R. M., Browne, R. W., Pidd, M., Williams, T., "A Measurement and Prediction Method for Determining Helicopter Noise Contours," 27th European rotorcraft Forum, Moscow, Sept 2001.

7. Schmitz, F. H., Ben, G. G., Sim, Wel-C, "Flight Path management and Control Methodology to Reduce Helicopter Blade-Vortex Interaction (BVI) Noise," AHS Vertical Lift Aircraft Design Conference, San Francisco, CA, Jan. 2000.

8. Conner, D.A., and Page, J.A., "A Tool for Low Noise Procedures Design and Community Noise Impact Assessment: The Rotorcraft Noise Model (RNM)," Presented at Heli Japan 2002, Tochigi, Japan, November 11-13, 2002.

9. Hardesty, M., Conner, D., Smith, C., and Terrell, W., "The Use of GPS Tracking and Guidance Systems for the Chicken Little Joint Project's 'Acoustic Week' Flight Test Program," AHS Forum 60, Baltimore, MD, June 7-10, 2004. In proceedings.

10. Page, J.A., "Simulation of Rotorcraft Noise including the Effects of Topography," Presented at the AHS International Technical Specialist Meeting on Aerodynamics, Acoustics, and Test and Evaluation, San Francisco, CA, January 23-25, 2002.

11. Rasmussen, K.B., "The Effect of Terrain Profile on Sound Propagation Outdoors", Danish Acoustical Institute Technical Report 111, January 1984.

12. Page, J.A., and Plotkin, K.J., "Acoustic Repropagation Technique Version 2 (ART2)," Wyle Research Report 01-04, January 2001.

13. Wilson, M., Mueller, A., and Rutledge, C., "A New Technique for Estimating Ground Footprint Acoustics for Rotorcraft Using Measured Sound Fields," Presented at the American Helicopter Society Vertical Lift Aircraft Design Conference, San Francisco, CA, Jan. 18-20, 1995.

14. Gray, D., Wright, K., and Rowland, W., "A Field-Deployable Digital Acoustic Measurement System," Technology 2000 Proceedings (published as NASA CP 3109, Vol. 2), Washington, DC, November 27-28, 1990, pp. 325–332.

15. Conner, D.A., "Measurement Resolution of Noise Directivity Patterns From Acoustic Flight Tests," NASA TM 4134, AVSCOM TP 89-B-004, October 1989

16. Brooks, T. F., and Burley, C. L., "Blade Wake Interaction Noise for a Main Rotor," Journal of the American Helicopter Society, Volume 49, Number 1, January 2004, pp 11-27.